1-1-1996

Characterization of the denaturation and renaturation of human plasma vitronectin I. Biophysical characterization of protein unfolding and multimerization

Ping Zhuang
The University of Tennessee, Knoxville

Michael N. Blackburn
GlaxoSmithKline plc.

Cynthia B. Peterson
The University of Tennessee, Knoxville

Recommended Citation

Zhuang, P., Blackburn, M., & Peterson, C. (1996). Characterization of the denaturation and renaturation of human plasma vitronectin I. Biophysical characterization of protein unfolding and multimerization. *Journal of Biological Chemistry, 271* (24), 14323-14332. https://doi.org/10.1074/jbc.271.24.14323

THE JOURNAL OF BIOLOGICAL CHEMISTRY
Vol. 271, No. 24, Issue of June 14, pp. 14323–14332, 1996

Printed in U.S.A.

Characterization of the Denaturation and Renaturation of Human Plasma Vitronectin

I. BIOPHYSICAL CHARACTERIZATION OF PROTEIN UNFOLDING AND MULTIMERIZATION*

(Received for publication, February 22, 1996, and in revised form, April 4, 1996)

Ping Zhuang‡, Michael N. Blackburn§, and Cynthia B. Peterson‡¶

From the ‡Department of Biochemistry and Cellular and Molecular Biology, University of Tennessee, Knoxville, Tennessee 37996 and the §Department of Macromolecular Sciences, SmithKline Beecham Pharmaceuticals, King of Prussia, Pennsylvania 19406

Upon treatment with denaturing agents, vitronectin has been observed to exhibit conformational alterations which are similar to the structural changes detected when vitronectin binds the thrombin-antithrombin complex or associates with the terminal attack complex of complement. Denaturation and renaturation of vitronectin isolated from human plasma were characterized by changes in intrinsic fluorescence. Unfolding by chemical denaturants was irreversible and accompanied by self-association of the protein to form vitronectin multimers. Self-association was evaluated by equilibrium analytical ultracentrifugation which demonstrated that multimers form only during the refolding process after removal of denaturant, that multimeric vitronectin dissociates to constituent subunits readily upon treatment with chemical denaturant, and that intermolecular disulfide cross-linking occurs primarily at the dimer level among a subset of constituent vitronectin subunits within the multimer. The monomeric form of vitronectin isolated from human plasma partially unfolds at intermediate concentrations of denaturant to an altered conformation with a high propensity to associate into multimers. Folding of vitronectin *in vivo* appears to be regulated by partitioning of folding intermediates toward either of two conformations, one that exists as a stable monomer and another that associates into a multimeric form.

Vitronectin is a plasma glycoprotein that is implicated as a regulator of diverse physiological processes, including blood coagulation, fibrinolysis, pericellular proteolysis, complement-dependent immune responses, and cell attachment and spreading (for reviews, see Refs. 1–5). The broad range in activities of vitronectin stems from its interaction with a wide variety of macromolecules, including zymogens, serpins, serpin-protease complexes, components of the membrane attack complex of complement, and mucopolysaccharides.

Quantification and detailed characterization of macromolecular ligand binding activities of vitronectin has been complicated by the fact that different molecular species of vitronectin are recovered from different purification protocols. The protein was first isolated by traditional biochemical approaches as S-protein, a species which associates with the terminal attack complex of complement and renders the complex soluble and unable to insert into target cell membranes (6, 7). This form of the protein has a molecular weight of approximately 72,000 and exists predominantly as a monomer. Higher yields of vitronectin were achieved using an alternative strategy for purification in which the protein is chemically denatured and isolated by affinity chromatography on a heparin column (8). The observation that vitronectin from denatured plasma bound to the heparin column, whereas binding of vitronectin from untreated, whole plasma was minimal, led to a model in which the heparin-binding site in vitronectin is cryptic in the native protein (9, 10). After quite some time it was realized that the heparin affinity-based purification of vitronectin yielded a high molecular weight form of the protein comprised of multiple vitronectin subunits (11, 12).

Chemical denaturation of vitronectin (13, 14), as well as macromolecular association with the thrombin-antithrombin III (13, 14) or the complement C5b-9 complex (12, 15), has been associated with a conformational transition of vitronectin to an altered form which is detected using monoclonal antibodies. Differences in functional reactivity of native and altered forms of vitronectin were initially demonstrated by changes in heparin-binding properties (13), and differences between the conformers have since been observed in interactions with plasminogen activator inhibitor type 1 (16–18), collagen (19), urokinase receptor (20), β-endorphin (15), and whole cells (21). Furthermore, different forms of vitronectin exhibit different efficiencies for incorporation into the extracellular matrix (22, 23). Indeed, immunological evidence suggests that this altered form of vitronectin, only detected in plasma in minor amounts, may be the predominant form of the protein found in extravascular sites (24).

Recently, attention has turned to structural characterization of the native and conformationally altered forms of vitronectin and the mechanism for conversion of the protein between alternative conformations. Initial demonstrations of altered immunoreactivity and heparin-binding properties were extended by Stockmann *et al.* (25), who demonstrated the propensity of vitronectin to self-associate into multimers upon treatment with chaotropes, detergents, extreme pH, or heat. Conformation-specific monoclonal antibodies were used extensively by these authors to demonstrate that structural alterations generally precede formation of the multimeric species with altered heparin binding. However, immunoreactivity varied according to individual epitopes recognized by monoclonal antibodies, as well as according to the stimulus used to induce self-association. A similar analysis of reactivity of native and heat-denatured vitronectin with a separate panel of monoclonal antibod-

* This work was supported by Grant HL50676 from the Heart, Lung and Blood Institute of the National Institutes of Health and by an Established Investigator Award from the American Heart Association (to C. B. P). The costs of publication of this article were defrayed in part by the payment of page charges. This article must therefore be hereby marked "*advertisement*" in accordance with 18 U.S.C. Section 1734 solely to indicate this fact.

¶ To whom correspondence should be addressed: M407 Walters Life Sciences Building, Dept. of Biochemistry and Cellular and Molecular Biology, University of Tennessee, Knoxville, TN 37996. Tel.: 423-974-4083; Fax: 423-974-6306; E-mail: Cynthia_Peterson@utk.edu.

ies also indicated structural alterations which are not limited to the heparin-binding region of the protein (26). Bittorf *et al.* (11) demonstrated an apparently irreversible conversion of vitronectin from a monomeric species to the oligomeric form to depend on the concentration of denaturant, with a transition in the range between 2 and 4 M urea. These *in vitro* studies point to the likelihood that conformationally altered forms of vitronectin found *in vivo* are also multimeric in nature.

A detailed analysis of the unfolding of vitronectin and refolding to a multimeric form is presented in this study, along with an evaluation of potential models for the mechanism of self-association of the protein in an accompanying report (27). Spectroscopic and hydrodynamic methods are used to evaluate structural changes which characterize unfolding and refolding of vitronectin. Particular attention is paid to the following questions. Is unfolding/refolding of native or multimeric vitronectin reversible? How do the different conformational forms of vitronectin differ according to secondary and tertiary structure? Do chemical denaturation and heat treatment of vitronectin yield the same conformer upon renaturation? To what extent is multimeric vitronectin stabilized by covalent intermolecular linkages?

EXPERIMENTAL PROCEDURES

Materials—Vitronectin was purified by a modification of the original procedure of Dahlback and Podack (7), essentially as described by Bittorf *et al.* (11). Purity was assessed by sodium dodecyl sulfate-polyacrylamide gel electrophoresis in the presence of β-mercaptoethanol (28). The molecular weight of the protein was determined to be 72,000 by equilibrium analytical ultracentrifugation (described below), and an extinction coefficient of 1.02 $ml \cdot mg^{-1} \cdot cm^{-1}$ was explicitly determined from the amino acid composition derived from a total amino acid hydrolysis on a protein sample of known absorbance. Multimeric vitronectin was prepared by treatment of protein in 8 M urea at room temperature for 2 h, with subsequent removal of denaturant by dialysis into standard phosphate buffer (0.1 M sodium phosphate, pH 7.5, containing 0.15 M NaCl, and 1 mM EDTA). Similar methods were used by both Stockmann *et al.* (25) and Bittorf *et al.* (11) to prepare the multimeric form of vitronectin. Heat-denatured vitronectin was prepared by incubating the protein in standard phosphate buffer at 55 °C for 2 h and subsequent cooling on ice (25, 26). Ultrapure guanidine hydrochloride was purchased from Life Technologies, Inc. Urea was a product of ICN biomedical. All other chemicals were of reagent grade quality.

HPLC[1] Analysis—Native and multimeric proteins were analyzed in standard phosphate buffer by HPLC using a Beckman ultraspherogel SEC2000 column (7.5 mm x 30 cm). Elution of protein from the column was monitored by absorbance at 280 nm. Retention times characteristic of native and multimeric vitronectin were 6.8 ± 0.1 and 5.6 ± 0.1 min, respectively.

Analytical Ultracentrifugation—Equilibrium sedimentation and sedimentation velocity measurements were performed with a Beckman XL-A analytical ultracentrifuge (Beckman Instruments, Spinco Division). Sedimentation equilibrium experiments were performed at approximately 20 °C using protein concentrations in the range of 0.1 to 0.3 $mg \cdot ml^{-1}$ in standard phosphate buffer or urea or GdnHCl in the same buffer. Data were collected after equilibrium had been established, generally after 18–24 h, using a rotor speed of 10,000 to 15,000 rpm for experiments on protein in buffer, or 48–72 h, with a rotor speed of 15,000 to 20,000 rpm, for experiments on protein in urea or GdnHCl.

The distribution of a single, homogeneous species within the ultracentrifuge cell at equilibrium is given by the equations:

$$c_r = c_m \exp(\sigma) + \text{base} \quad \text{(Eq. 1)}$$

$$\sigma = M(1 - \bar{v}\rho)\omega^2(r^2 - r_m{}^2)/2RT \quad \text{(Eq. 2)}$$

in which c_r and c_m are the concentrations of the protein at radial position, r, and at a reference position, r_m (*i.e.* the meniscus), respectively. M is the protein molecular weight, $\bar{v}$ is the partial specific volume, equal to 0.73 $ml \cdot g^{-1}$, ω is the angular velocity, R is the gas constant, T is absolute temperature, and base is a term for non-sedimenting baseline absorbance. Solvent density, ρ, was estimated to be 1.018 for the buffer, and the density of guanidine or urea solutions was calculated according to Kawahara and Tanford (29). For the analysis of samples containing multiple sedimenting species, *e.g.* monomer, dimer, etc., the concentration distribution can be written as the sum of the distributions for the individual species, i, as:

$$c_r = \sum c_{m,i} \exp(\sigma_i) + \text{base} \quad \text{(Eq. 3)}$$

Data were analyzed using nonlinear least squares methods, as described by Brooks *et al.* (30, 31), using IGOR (Wavemetrics, Lake Oswego, OR) on a Macintosh computer.

Sedimentation velocity data were likewise analyzed using the IGOR software package. After reaching full centrifugation speed of 60,000 rpm, data sets were collected at 4–8-min intervals, with at least 10 data sets collected per run. The sedimentation coefficient, $s_{20,w}$, was determined from the slope of a plot of $\ln r_m$ *versus* $\omega^2 t$.

Spectroscopic Analysis of Chemical Denaturation of Vitronectin—Unfolding of vitronectin was induced by GdnHCl or urea and monitored by changes in intrinsic protein fluorescence. Protein fluorescence measurements were made on a Perkin-Elmer LS-50B spectrofluorimeter. Emission spectra were recorded between 300 and 450 nm using an excitation wavelength of 290 nm and a pathlength of 1 cm. Changes in emission spectra were quantified as the average emission wavelength, which was calculated according to the following expression:

$$\bar{\lambda} = \frac{\sum \lambda_i I_i}{\sum I_i} \quad \text{(Eq. 4)}$$

where λ_i and I_i are the emission wavelength and its corresponding fluorescence intensity at that wavelength (32). To facilitate comparison between different experiments, the average emission wavelength at any denaturant concentration is converted to F_{app}, the fraction of unfolded protein, by the equation $F_{app} = (\lambda_{obs} - \lambda_F)/(\lambda_U - \lambda_F)$ in which λ_F and λ_U are the average emission wavelengths associated with folded and unfolded proteins, respectively. Buffer used for the unfolding and refolding experiments was standard phosphate buffer containing 0.04% Tween 20. GdnHCl and urea concentrations were calculated using equations relating refractive indexes to concentrations (33), and refractive indexes were measured using a Zeiss refractometer. Urea solutions were made fresh daily.

Quenching of tryptophan fluorescence was performed by addition of sodium iodide as described by Lakowicz (34). Sodium iodide was dissolved in standard phosphate buffer to a final concentration of 5 M, and aliquots were added to solutions of vitronectin (0.1 μM) in standard phosphate buffer or 7 M GdnHCl. The excitation wavelength was 290 nm, and emission was measured at the maximum wavelength observed in the emission spectra, 340, 351, and 350 nm, for native, multimeric, or fully denatured protein, respectively.

Circular dichroism measurements were made on a Jasco Model J710 Spectrapolarimeter at 22 °C using a cell with a pathlength of 0.02 cm. The average of four accumulations is reported, using a 1-nm band width, 1-nm step resolution, 50 $nm \cdot min^{-1}$ scan rate, and 2-s response time. Instrument sensitivity was set at 20 millidegrees. Protein concentration was 0.95 $mg \cdot ml^{-1}$ in 0.1 M sodium phosphate, pH 7.5, containing 0.15 M NaCl. Spectra were collected for protein in buffer and protein in buffer plus 6.5 M GdnHCl under the same conditions. A mean residue molecular weight of 113.8 was used.

RESULTS

Unfolding of Vitronectin Can be Monitored by Changes in Secondary or Tertiary Structure—Studies of protein folding generally rely on one or more probes of structure and function, monitoring changes in those parameters as denaturation conditions are varied. In order to more fully characterize the unfolding transition of vitronectin, spectroscopic methods were evaluated to reliably monitor structural alterations which accompany the unfolding transition for this particular protein. Fig. 1 shows far UV circular dichroism spectra for vitronectin under native and highly denaturing (6.5 M GdnHCl) conditions. The spectrum for the native protein, which has been reported by Pitt *et al.* (35), exhibits a gradual slope from approximately 230 nm, with a trough near 205 nm. This spectrum is characteristic of a protein with predominant β-sheet and random fold

[1] The abbreviations used are: HPLC, high performance liquid chromatography; GdnHCl, guanidine hydrochloride; PAGE, polyacrylamide gel electrophoresis.

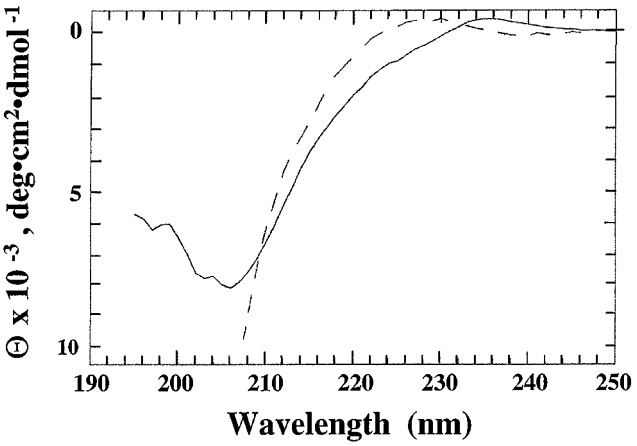

FIG. 1. **Near-UV circular dichroism spectra for native and denatured vitronectin.** Vitronectin was diluted to a concentration of 0.95 mg·ml^{-1} in 0.1 M sodium phosphate buffer, pH 7.5, containing 0.15 M NaCl (*solid curve*) or approximately 6.5 M GdnHCl in the same buffer (*dashed curve*). Spectra were recorded on samples in a circular quartz cell with a 0.02-cm pathlength. The spectra shown have been corrected for any ellipticity measured on buffer or denaturant alone. The spectrum in GdnHCl is shown only for wavelengths at which the high voltage on the photomultiplier tube was less than 500 volts.

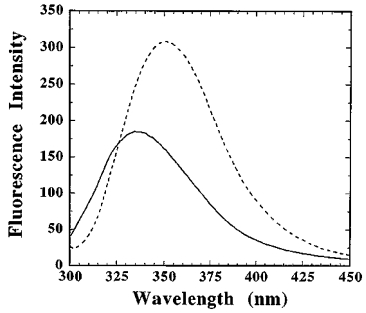

FIG. 2. **Fluorescence emission spectra for native and denatured vitronectin.** Vitronectin was diluted to a concentration of 0.5 μM in 0.1 M sodium phosphate buffer, pH 7.5, containing 0.15 M NaCl, 1 mM EDTA, and 0.04% Tween 20 (*solid line*) or 7 M GdnHCl in the same buffer (*dashed line*). Excitation was at 290 nm, and spectra were recorded 16 h following addition of the protein to buffer or denaturant.

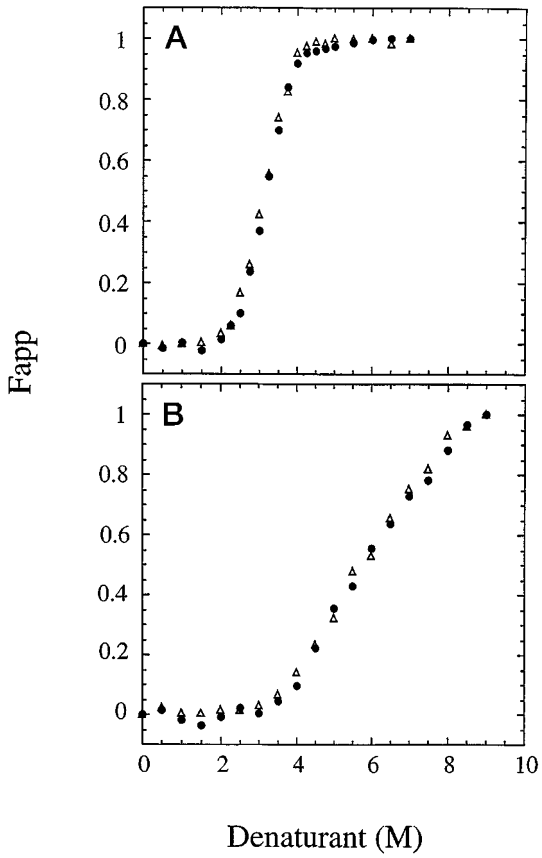

FIG. 3. **Unfolding curves for vitronectin measured by changes in intrinsic fluorescence.** Unfolding of purified native vitronectin in GdnHCl (*panel A*) or urea (*panel B*) was monitored by average tryptophan emission wavelength, as described under "Experimental Procedures." Following overnight incubation of vitronectin at each concentration of denaturant in buffer, emission spectra were recorded from 300 to 450 nm using an excitation wavelength of 290 nm. In both panels, data for 0.5 μM vitronectin are described by ●, and data for 5 μM vitronectin by Δ. Data are expressed as F_{app}, the apparent fraction unfolded, by normalization of individual readings to λ_F and λ_U as given in Table I.

character, with little α-helical content.[2] The spectrum for denatured vitronectin exhibits loss of negative ellipticity in the 215–230 nm region, with a concomitant increase in negative ellipticity in the vicinity of the 205-nm trough. Spectra could not be accurately measured below 207 nm on protein samples in denaturant solutions due to absorption of guanidine.

Intrinsic fluorescence of vitronectin was also perturbed upon chemical denaturation (Fig. 2). Denaturation of vitronectin is associated with an increase in quantum yield, along with a red shift in emission maximum, expected upon exposure of buried tryptophan residues to a more hydrophilic environment upon unfolding. Changes observed in both circular dichroism and fluorescence indicate loss of secondary and tertiary structure upon chemical denaturation. Since accurate measurements cannot be obtained by CD due to absorption by the denaturant in the region where ellipticity changes appear to be the greatest, detailed characterization of the unfolding transition of vitronectin was pursued exclusively using the fluorescence method.

Denaturation of Vitronectin by Chemical Treatment Is not Accompanied by Aggregation—Changes in fluorescence emission maxima for vitronectin were monitored as a function of chemical denaturant using either GdnHCl (Fig. 3*A*) or urea (Fig. 3*B*). Unfolding of vitronectin in GdnHCl occurs at a lower concentration of denaturant than in urea, with midpoints of 3.2 M and 5.9 M denaturant, respectively. The unfolding transition of vitronectin occurs over a narrow concentration range in GdnHCl, compared to the more gradual denaturation observed over the broad range from 3 to 9 M urea. The unfolding curves in either chemical denaturant are indistinguishable for vitronectin concentrations varied over a 10-fold range (Fig. 3), indicating that there are no association or dissociation phenomena which accompany unfolding of the protein. Table I lists the midpoints for denaturation of vitronectin measured for both denaturants using different protein concentrations.

The aggregation state of vitronectin in the presence and absence of chemical denaturants was evaluated by sedimentation equilibrium in an analytical ultracentrifuge. This technique is considered to be the most reliable for determining molecular weight and is ideally suited for examining association and dissociation phenomena. Fig. 4*A* shows a representative data set with a diagnostic distribution of native protein at equilibrium from the meniscus, which is depleted of protein, to the bottom of the centrifugation cell, which contains a high concentration of protein. The smooth curve represents a fit to a single species, which yielded a molecular weight of 73,800 for this data set, and residuals shown in Fig. 4*B*. The homogeneity

[2] The CD spectrum for the multimeric form of vitronectin does not differ substantially in overall shape from that recorded for the native, monomeric protein.

TABLE I
Behavior of native and multimeric vitronectin in chemical denaturation/renaturation experiments

Vitronectin sample[a]	Denaturant	Midpoint (M)	$\bar{\lambda}_F$[b]	$\bar{\lambda}_U$[b]
Unfolding conditions				
0.5 μM native	GdnHCl	3.2	349.7	363.8
5.0 μM native	GdnHCl	3.2	349.7	363.9
0.5 μM native	Urea	5.9	350.0	360.2
5.0 μM native	Urea	5.9	350.6	360.4
0.5 μM multimer	GdnHCl	2.2	352.2	360.0
5.0 μM multimer	GdnHCl	2.1	351.8	360.4
0.5 μM heat-treated	GdnHCl	2.6	351.9	361.9
Refolding conditions[c]				
0.5 μM native	GdnHCl	2.1	352.1	360.7
0.5 μM native	Urea	4.8	353.2	361.1
0.5 μM multimer	GdnHCl	2.1	352.7	360.1
0.5 μM heat-treated	GdnHCl	2.6	352.1	362.3

[a] Samples are labeled according to the state of the starting material for the experiment as: native, corresponding to the untreated monomeric protein; multimeric, corresponding to the chemically denatured then renatured form of the protein; and heat treated, corresponding to the protein heated to 55 °C as described under "Experimental Procedures."

[b] The intensity averaged wavelength corresponding to folded, *F*, or unfolded, *U*, protein. Error limits on these measurements are ± 0.2 nm.

[c] For refolding experiments, protein was initially denatured in either 7 M GdnHCl or 9 M urea, as designated, for 16 h. The vitronectin sample types listed thus correspond to the starting material which was initially denatured prior to the refolding experiment.

of the sample is noteworthy, with no evidence for even small amounts of multimeric vitronectin in the preparation.

Data from a representative equilibrium centrifugation experiment on vitronectin unfolded in a high concentration of GdnHCl is shown in Fig. 4*C*, again with a smooth curve through the data representing a fit to a single species of molecular weight 70,900 and the residuals of the fit shown in Fig. 4*D*. Clearly, there is no association of vitronectin to form multimers in the presence of GdnHCl, as not even a small amount of high molecular weight protein is detected by this method. Sedimentation velocity experiments at 60,000 rpm were used to verify this conclusion; at these high centrifugation speeds, there were no faster sedimenting species and the unfolded monomer was observed as the only form of vitronectin present (data not shown). Table II summarizes results from equilibrium sedimentation analysis of vitronectin, using a variety of experimental conditions.

Chemical Denaturation of Vitronectin Is Not Readily Reversible—Early in the work evaluating chemical denaturation of vitronectin, it was observed that unfolding of the protein occurs on an extremely slow time scale. Precautions were observed to establish that equilibrium had been reached in the denaturation process since one of the original goals for this study was to evaluate the thermodynamics of unfolding of vitronectin. The kinetics of unfolding of vitronectin at two different concentrations of denaturant are shown in Fig. 5. As expected, the slowest rate of unfolding is observed at denaturant concentrations close to the midpoint in the unfolding curve. Unfolding is complete only after chemical treatment for many hours, with small changes in fluorescence at 3 M GdnHCl observed even up to 24-h incubation times. Extremely slow unfolding has been observed with other proteins and has in some cases confused interpretation of energetics of unfolding (36, 37).

For this reason, equilibrium unfolding of vitronectin was explicitly tested by evaluating the reversibility of the chemically-induced unfolding reaction. Refolding of vitronectin was measured by first treating the protein with high concentrations of chemical denaturant for 16 h and then allowing refolding to proceed in varying mixtures of denaturant and buffer for long time periods. The refolding behavior exhibited by vitronectin treated with GdnHCl and urea is plotted, along with the unfolding curves measured in both chemical denaturants, in Fig. 6. Hysteresis in refolding *versus* unfolding curves is observed with both types of denaturants, with the most pronounced differences exhibited for GdnHCl treatment.[3] The non-identical nature of the unfolding and refolding curves for vitronectin indicates either that unfolding and refolding proceed by different pathways, or that the starting and ending protein species are chemically distinct. Table I summarizes the results from the unfolding and refolding studies performed on vitronectin with both GdnHCl and urea, including the midpoints for the denaturation curves and the intensity-averaged emission wavelengths for the folded and unfolded proteins, λ_F and λ_U, respectively.

Refolding of Vitronectin Is Accompanied by Self-association into Multimers—Recent reports have indicated that vitronectin has a tendency to self-associate in a concentration-dependent manner following chemical or heat denaturation. Therefore, an obvious possibility which would account for hysteresis in unfolding and refolding is that the protein refolds in a manner that promotes oligomerization. Chemically denatured and subsequently renatured vitronectin was analyzed according to size by the sedimentation equilibrium method, and the results are shown in Fig. 7*A*. An average molecular weight of approximately 420,000 can be derived for renatured vitronectin, although the data cannot be fit to a single species. This result corroborates independent work from the laboratories of Preissner (25) and Mosher (11) which indicates that vitronectin multimers may range in size from multiples of 3 to 16 monomers. This molecular weight is somewhat lower than that for multimeric vitronectin estimated previously by either Bittorf *et al.* (11) or Stockmann *et al.* (25). However, the molecular weight of 790,000 given for the multimer by Bittorf and co-workers was calculated for a multimer isolated directly from plasma using denaturing conditions modified from the original protocol of Yatohgo (8), and these authors indicate that they generate a multimer of somewhat lower molecular weight when vitronectin is first isolated from plasma in a native form and then denatured. Sedimentation velocity experiments on multimeric vitronectin yielded a broad sedimenting boundary corresponding to a sedimentation coefficient of 11 S, compared to a sedimentation coefficient of 4.1 S for native vitronectin (Table II).

Denaturation of multimeric vitronectin using GdnHCl resulted in a strikingly different unfolding curve compared to that observed for native, monomeric protein (Fig. 8), indicating the multimeric species is less resistant to chemical denaturation. Multimeric vitronectin unfolds with a midpoint of 2.1 M GdnHCl, while native protein has a midpoint of 3.2 M GdnHCl. Moreover, unfolding and refolding curves for the multimeric form of the protein are superimposable (Fig. 8), indicating reversibility of chemical denaturation of this protein. The denaturation/renaturation curves are indistinguishable from the refolding behavior exhibited subsequent to denaturation of native vitronectin (Fig. 6), which was noted above by its hysteretic relationship to unfolding of monomeric protein. Similar behavior is observed upon denaturation of the protein with urea. Note that values for λ_F and λ_U are the same for unfolding and refolding for the multimer, as would be expected for a reversible reaction (Table I). Also, the kinetics of unfolding of mul-

[3] Indeed, the marked dissimilarity observed between unfolding and refolding of vitronectin in GdnHCl spurred our re-evaluation of earlier data in urea (40), in which the observed differences were not as obvious, and supported the interpretation that observed variations represent true differences in unfolding and refolding patterns rather than imprecision in measurements.

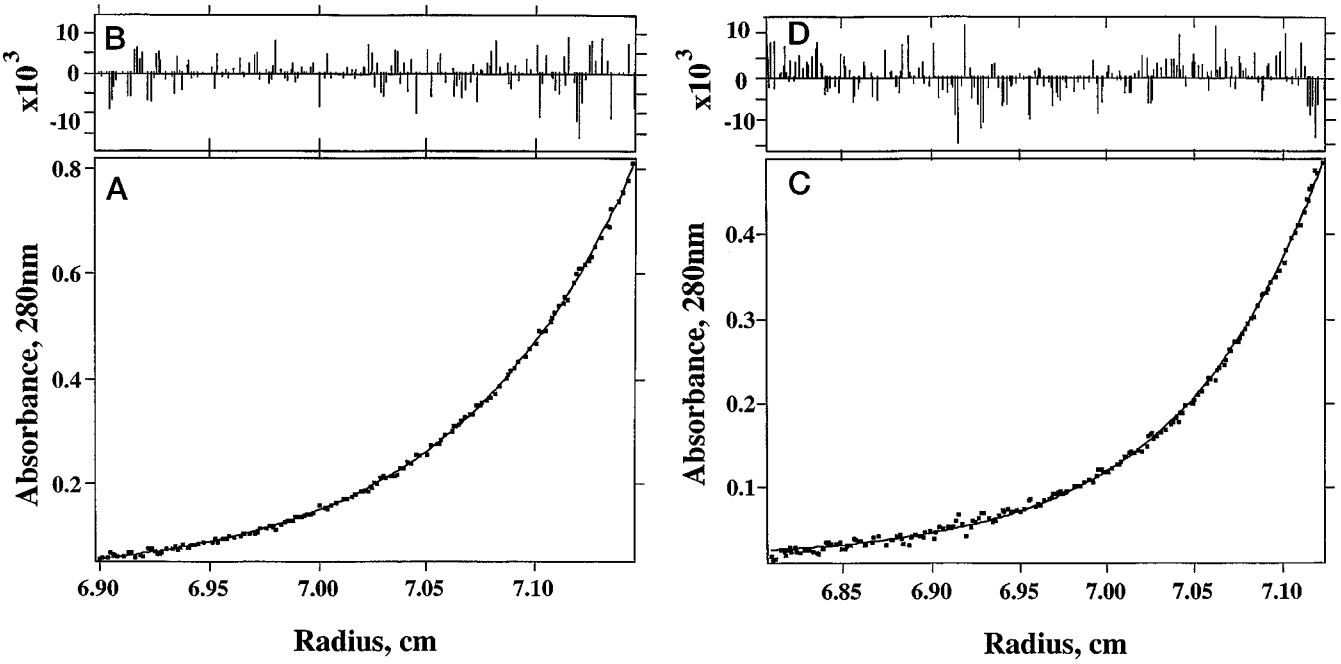

FIG. 4. **Equilibrium analytical centrifugation on the vitronectin monomer using native or denaturing conditions.** *Panel A* shows the radial distribution of absorbance in the centrifuge cell at equilibrium at 15,000 rpm for native vitronectin at a concentration of 0.3 mg·ml^{-1} in 0.1 M sodium phosphate, pH 7.5, 0.15 M NaCl. Individual absorbance readings are shown by *closed squares*, with a *solid line* through the data representing the fit to a single species of molecular weight equal to 73,800. The residuals for the fit are shown in *panel B. Panel C* shows the distribution of absorbance in the cell after reaching equilibrium with a centrifugation speed of 20,000 rpm for native vitronectin (0.22 mg·ml^{-1}) unfolded in 6.53 M GdnHCl. Absorbance data points are shown in *solid squares* and the *smooth curve* through the data represents the best fit to a single species model, yielding a molecular weight of 70,900. Residuals for the fit are shown in *panel D*.

TABLE II
Molecular weight determinations for vitronectin samples under native and denaturing conditions

Vitronectin sample[a]	Solvent	Sedimentation velocity experiments, $s_{20,w}$	Sedimentation equilibrium experiments	
			M_r	Average M_r
Native	PBS[b]	4.1 S	72,400	73,100
Native	Buffer[c]		73,800	
Native	8.76 M Urea		77,300	73,700
Native	8.02 M Urea		70,100	
Native	7.08 M GdnHCl		71,300	
Native	6.53 M GdnHCl		70,900	70,600
Native	5.98 M GdnHCl		69,700	
Multimer	Buffer[c]	11 S	~420,000	
Multimer	6.0 M GdnHCl		~70% Monomer, M_r = 72,000 ~30% Disulfide-linked species	
Heat-treated	Buffer[c]	22 S		

[a] Samples are labeled according to the state of the starting material for the experiment as: native, corresponding to the untreated monomeric protein; multimeric, corresponding to the chemically denatured then renatured form of the protein; and heat treated, corresponding to the protein heated to 55 °C as described under "Experimental Procedures."
[b] Phosphate-buffered saline (40 mM sodium phosphate, pH 7.4, containing 0.15 M NaCl).
[c] Unless otherwise noted, buffer is standard phosphate buffer.

timeric vitronectin are more rapid than observed with native protein, as shown in the *inset* to Fig. 8. These observations indicate that, following denaturation of native, monomeric vitronectin, the protein refolds and assumes an altered tertiary structure with less stability to chemical denaturants.

The tertiary structure of vitronectin was assessed by measuring the susceptibility of different forms of the protein to quenching of intrinsic fluorescence with iodide. Stern-Volmer plots of quenching behavior observed for native protein, fully denatured vitronectin in 7 M GdnHCl, and renatured, multimeric vitronectin are shown in Fig. 9. Not surprisingly, the fully unfolded protein is more susceptible to chemical quenching, with the tryptophan fluorophores more highly exposed to solvent in a non-native structure. Iodide quenching observed for the native protein corresponds to an average of 70% exposure of tryptophans to solvent, whereas the quenching curve measured for vitronectin in the presence of 7 M GdnHCl corresponds to essentially 100% exposure (20). Refolded, multimeric vitronectin exhibits quenching behavior which is intermediate between that observed for native, monomeric protein and the fully denatured form of the protein. Tryptophans in the multimeric protein are obviously in different environments upon refolding and self-association, with a much higher susceptibility to quenching compared to tryptophans in native vitronectin, supporting the contention that a different tertiary fold has been assumed upon renaturation.

Multimeric Vitronectin Dissociates into Subunits Prior to Unfolding of Polypeptide Chains upon Chemical Denaturation—As already discussed (Fig. 7*A*), equilibrium analytical ultracentrifugation of multimeric vitronectin gave no evidence of dissociation to monomeric forms in buffer, indicating that the native and multimeric forms of the protein are not in

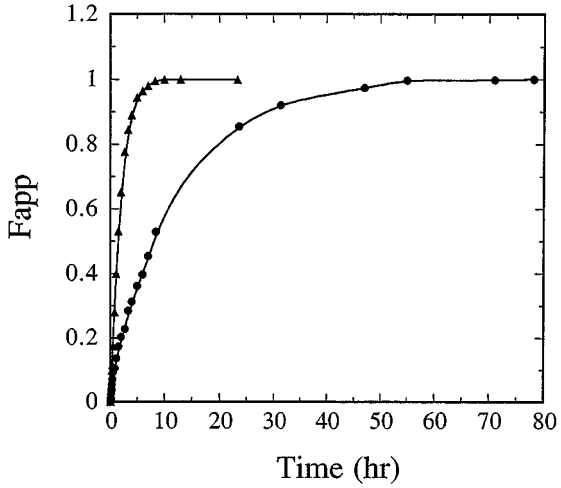

FIG. 5. **Kinetics of unfolding of vitronectin in GdnHCl.** Unfolding of vitronectin was monitored at various time points by the intensity-averaged tryptophan emission wavelength. Data are shown for a concentration of 3 M GdnHCl (*i.e.* the midpoint in the denaturation curve shown in Fig. 3) with the *solid circles* and for a concentration of 4 M GdnHCl with the *solid triangles*. Data are expressed as F_{app}, the apparent fraction unfolded, by normalization of individual readings to λ_F and λ_U as given in Table I.

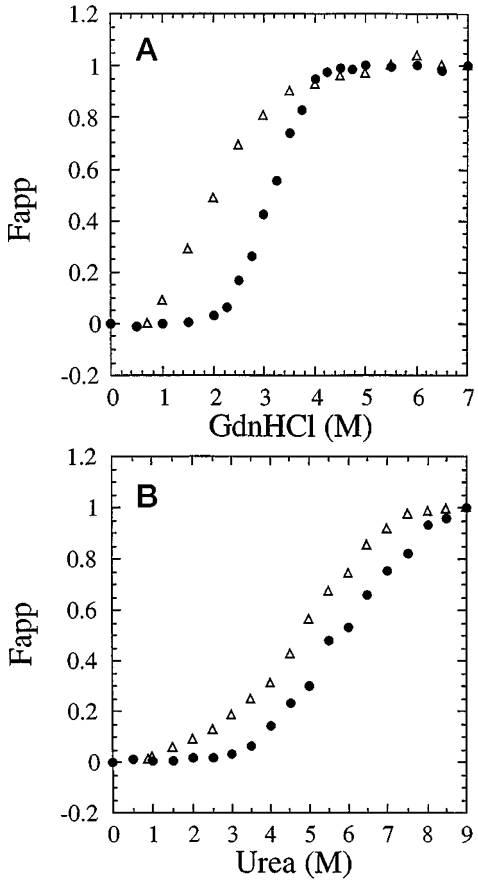

FIG. 6. **Hysteresis in unfolding and refolding curves for vitronectin.** The extent of unfolding (●) and refolding (Δ) of 0.5 μM vitronectin was monitored by intensity-averaged emission wavelength using GdnHCl (*panel A*) or urea (*panel B*) as the denaturant. Data are expressed as F_{app}, the apparent fraction unfolded, by normalization of individual readings to λ_F and λ_U as given in Table I to facilitate comparison between unfolding and refolding data. For refolding data, proteins were initially denatured overnight in 7 M GdnHCl (*panel A*) or 9 M urea (*panel B*), and then refolding was achieved by diluting out denaturant with buffer at intermediate concentrations up to a 10-fold dilution and incubating for 16 h. Refolding in GdnHCl (*panel A*) was not measured below 0.7 M GdnHCl, but the λ_F was determined following dialysis to remove all denaturant. The value for λ_F given in Table I at 0.0 M denaturant is the same as the value measured in 0.7 M GdnHCl.

equilibrium. Interconversion between multimeric and monomeric forms was also not observed in analytical gel filtration HPLC experiments in which the multimeric protein exhibited no tendency to dissociate in buffer, even after incubation at room temperature for greater than 24 h. Furthermore, size exclusion chromatography on mixtures of native and multimeric protein in defined ratios resulted in elution of well separated peaks corresponding to multimeric and monomeric protein, with peak areas proportional to starting amounts of each protein species.

However, the average molecular weight of multimeric vitronectin decreases upon treatment with high concentrations of GdnHCl or urea, corresponding to dissociation of multimers into constituent monomers. Dissociation of the multimer upon chemical denaturation was demonstrated by equilibrium analytical ultracentrifugation, with a sample data set shown in Fig. 7*B* and results summarized in Table II. Adequate fitting of the ultracentrifugation data was achieved only by considering a mixture of species which corresponds to monomers of average molecular weight near 72,000, along with a component of disulfide cross-linked species. Fitting of the data in 6.5 M GdnHCl to this model, along with deconvolution into contributions from the two molecular species, is shown in Fig. 7*B*. The dimer component was disrupted by treatment of the protein mixture with high concentrations of reducing agent (10 mM dithiothreitol), and a single species of molecular weight equal to the monomer was observed in 6.5 M GdnHCl under those conditions. Some analyses on denatured multimer also indicate a variable contribution from disulfide cross-linked species of higher order than dimers, although adequate fits of the data do not consistently require their inclusion. Previous work has demonstrated that denaturation of vitronectin is accompanied by disulfide rearrangement (13, 14) and some stabilization of multimers by disulfide cross-links has been proposed (11, 25). Evaluation of the ultracentrifugation results definitively demonstrates that the multimeric species is not uniformly stabilized by these covalent intermolecular cross-links, as the majority of multimeric species dissociate into monomers upon denaturation.

In spite of the clear demonstration that multimeric vitronectin dissociates into constituent monomers (and a disulfide cross-linked component) upon denaturation, varying protein concentration over a 10-fold range does not affect GdnHCl unfolding curves (Fig. 8). In cases in which dissociation accompanies unfolding, theory would predict that there should be a strong concentration dependence in unfolding curves due to the change in the molecularity of the folded and unfolded species, and experiments have substantiated this prediction in many systems (see Ref. 38 and references therein). Lack of protein concentration dependence in the unfolding of multimeric vitronectin upon chemical denaturation is therefore surprising. Analytical ultracentrifugation was used to evaluate dissociation of the multimer at various denaturant concentrations in order to determine whether dissociation precedes unfolding, or whether it occurs concomitantly with unfolding of constituent polypeptide chains. Fig. 10 shows a comparison of dissociation of multimeric vitronectin and the unfolding curve observed with fluorescence at concentrations of GdnHCl between 0 and 7 M GdnHCl. There is a striking difference between the two relationships which indicates that multimeric vitronectin dissociates at low concentrations of denaturant, prior to unfolding of constituent polypeptide chains. There appears to be little contribution to observed changes in fluorescence upon denatur-

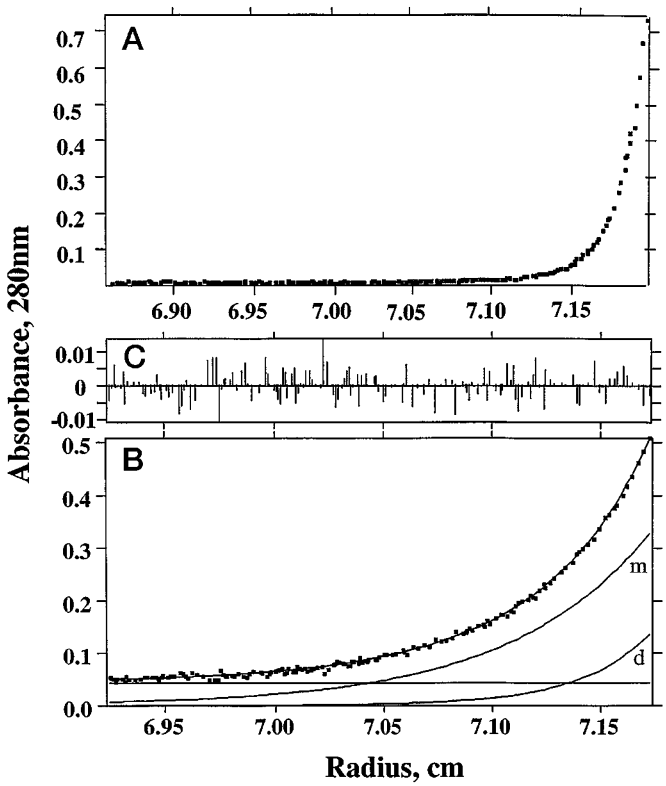

FIG. 7. **Equilibrium analytical ultracentrifugation on multimeric vitronectin under native and denaturing conditions.** *Panel A* shows the distribution of absorbance along the centrifugation axis within the ultracentrifuge cell at equilibrium at 10,000 rpm for the multimeric form of vitronectin at a concentration of 0.1 mg·ml^{-1} in 0.1 M sodium phosphate, pH 7.5, containing 0.15 M NaCl. *Panel B* shows the distribution of absorbance at equilibrium at 20,000 rpm for multimeric vitronectin in 6.5 M GdnHCl. Data points are shown in the *solid squares*, and the *smooth curve* through the data represents a fit to a model assuming a mixture of monomers and dimers, with a monomer molecular weight of 72,000. Deconvolution of the individual contributions of monomer and dimer are shown by the *solid lines* denoted *m* and *d*, respectively. The residuals of the fit to the two-species model are shown in *panel C*.

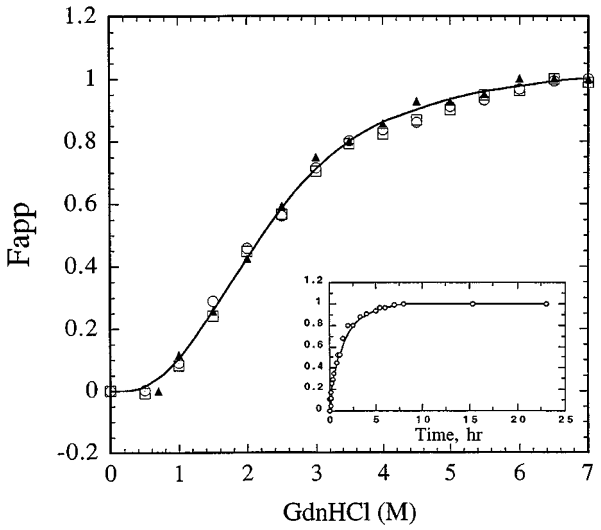

FIG. 8. **Equilibrium unfolding and refolding of multimeric vitronectin.** Unfolding of multimeric vitronectin at a concentration of 0.035 mg·ml^{-1} (○) or 0.35 mg·ml^{-1} (□) in GdnHCl was monitored by fluorescence as the intensity-averaged emission wavelength. Data are also shown for refolding of 0.035 mg·ml^{-1} multimeric vitronectin (▲) after unfolding for 16 h in 7 M GdnHCl. The *inset* shows the kinetics of unfolding using a concentration of 2.6 M GdnHCl, which corresponds to the midpoint in the unfolding/refolding curves. Data on the *y* axis are all expressed as F_{app}, the apparent fraction unfolded, by normalization of individual readings to λ_F and λ_U as given in Table I.

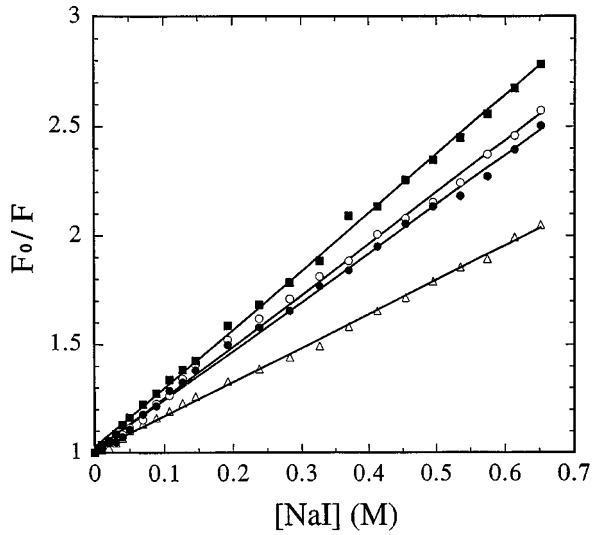

FIG. 9. **Stern-Volmer plot for iodide quenching of various folded forms of vitronectin.** Data are shown for the native monomer (Δ) in buffer, fully denatured monomer (■) in 7 M GdnHCl, multimeric vitronectin (●) in buffer, and heat-treated vitronectin (○) in buffer.

ation that can be attributed to dissociation alone. Thus, the lack of protein concentration dependence for unfolding of multimeric vitronectin monitored by fluorescence is attributed to the fact that dissociation occurs prior to any substantial unfolding.

Heat-denatured and Chemically Denatured Vitronectin Are Not Structurally Identical—Denaturation of vitronectin has been pursued by different research groups using different methods, most commonly by treatment with either heat or chaotropic agents, to produce functionally and structurally altered protein. From characterization of alterations in mobility on native and non-reducing SDS gels, comparison of ligand binding properties, and reactivity with a limited number of monoclonal antibodies, it has been tentatively assumed by some that the altered forms of vitronectin produced by thermal and chemical denaturation are similar in function. The biophysical analyses developed for characterization of chemical denaturation of vitronectin offered the possibility of comparing molecular size, fluorescent properties, and stability of the renatured proteins that were unfolded thermally or with chaotropes. Sedimentation velocity measurements demonstrated a larger average size of vitronectin multimers generated by heat denaturation compared to those produced by chemical denaturation, with heat-treated multimers sedimenting at 22 S *versus* 11 S, as observed for vitronectin renatured following denaturing with urea (Table II). In a comparison of many different denaturing conditions in effecting self-association of vitronectin, Stockmann *et al.* (25) noted that elevated temperatures produce multimeric species with higher molecular weights apparent from their decreased permeability into polyacrylamide gels.

Multimeric forms of vitronectin generated by thermal and chemical denaturation were compared in terms of their stability toward GdnHCl-induced unfolding. Fig. 11 shows unfolding curves monitored by changes in intrinsic protein fluorescence for both forms of multimeric vitronectin, along with the unfolding curve characteristic of native, monomeric protein for reference. Differences between unfolding of the two multimeric forms are observed in the midpoints in the denaturation curves and from the different shapes of the two unfolding curves, with the heat-treated protein exhibiting a sharper transition than

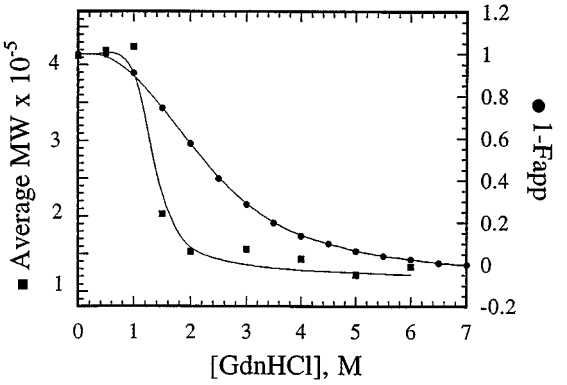

FIG. 10. **Dissociation and unfolding of multimeric vitronectin by GdnHCl.** The average molecular weight of the vitronectin sample (shown by the *solid squares*) was calculated from equilibrium analytical sedimentation runs at various concentrations of GdnHCl. Unfolding of the multimer (shown in the *solid circles*) was followed by fluorescence calculated as the intensity-averaged emission wavelength. Unfolding is expressed as $1 - F_{app}$, *i.e.* the fraction folded, *versus* denaturant concentration. F_{app} is calculated by normalization of individual readings to λ_F and λ_U as given in Table I. *Smooth lines* through the data are for presentation purposes only and do not represent fits to a particular model.

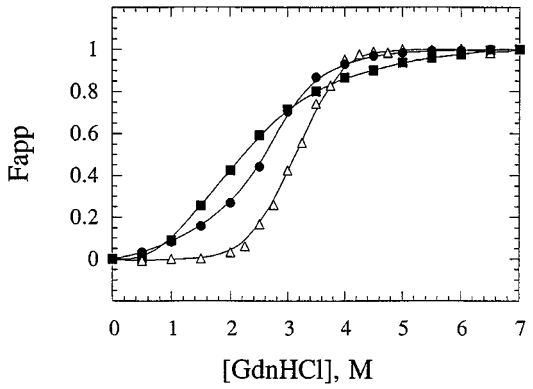

FIG. 11. **Unfolding curves compared for native, multimeric, and heat-denatured vitronectin.** Fluorescence emission data were recorded at varying GdnHCl concentrations for 0.035 mg·ml^{-1} native (Δ), multimeric (■), or heat-denatured (●) vitronectin. Unfolding was monitored by changes in the intensity-averaged emission wavelength and is normalized to F_{app}, the fraction unfolded, at a given denaturant concentration to facilitate comparison of the three data sets. F_{app} is calculated by normalization of individual readings to λ_F and λ_U as given in Table I. *Smooth lines* through the data are for presentation purposes only and do not represent fits to a particular model.

the gradual unfolding over a broad range in denaturant exhibited by the chemically-induced multimer. Since the multimeric form of vitronectin dissociates at relatively low concentrations of denaturant into its constituent subunits, the unfolding curves are thought to primarily characterize unfolding of the monomeric subunits within the multimer. Observed differences in the unfolding curves thus presumably reflect altered folding and stability of the component protein chains. Clearly, the differences in size, fluorescent properties, and sensitivity to chemical denaturants demonstrate that the heat-treated multimer is not folded identically to the multimeric form of vitronectin generated by chemical denaturation and subsequent renaturation. These differences should be considered by other investigators comparing functional properties of native and multimeric vitronectins. Indeed, it is not clear at this point whether the heat-treated or chemically-treated form of vitronectin represents a better model for multivalent vitronectin species which apparently exist *in vivo*.

DISCUSSION

Attention has been paid to evaluating the effects of urea on the structure and function of vitronectin since it was noted that reactivity with a conformation-specific monoclonal antibody (8E6, see Refs. 13 and 14) was increased by urea treatment in a manner reminiscent of conformational changes that are induced in vitronectin by interactions with more physiologically relevant molecules, including the thrombin-antithrombin complex and the C5b-9 complex. The purpose of this study was to evaluate *in vitro* effects of denaturation on the overall fold of vitronectin in order to understand the conformational lability that the protein appears to exhibit *in vivo*. For this reason, the investigation was initiated using some of the strategies which have proven useful to the general field of protein folding as it has emerged over the last 30 years. A first approach was to determine whether chemical denaturants could be used to unfold and subsequently refold vitronectin in a reversible fashion so that some insight could be gained into the intrinsic stability and energetic differences between different conformational forms.

Unfolding of vitronectin was most readily monitored over a wide range of denaturant concentrations by using the 9 tryptophans within the protein as intrinsic fluorescent probes, sensitive to the protein environment in a variety of different vicinities within the global fold. Upon denaturation, the fluorescence of the protein increased, indicating that tryptophans are quenched in their native environments within the tertiary structure of vitronectin. By monitoring changes in the fluorescence of the protein, highly reproducible unfolding curves were observed for vitronectin treated with varying concentrations of either GdnHCl or urea. Bittorf *et al.* (11) evaluated changes in several properties of vitronectin following treatment with urea. Alterations of immunoreactivity with antibody 8E6, increased binding to heparin, formation of multimeric species, and sulfhydryl rearrangement were all observed upon treatment of vitronectin with a critical concentration of at least 2–2.5 M urea. Response curves for each of these criteria *versus* molar urea concentration were similar, although not identical. Midpoints for the expression of altered properties measured by Bittorf *et al.* (11) were generally observed at concentrations between 2 and 3.5 M urea, whereas the midpoint for disruption of the overall tertiary structure of vitronectin in this work was observed at greater than 5 M urea. Part of the disparity between the different experiments may be attributed to the long unfolding times used in this work, as compared to a 2-h unfolding interval used by Bittorf and co-workers. However, the observation that altered immunoreactivity and a tendency toward formation of multimers occur at *lower* concentrations of urea and shorter unfolding times than the more generalized unfolding of the protein chain supports the notion of a partially folded intermediate form of vitronectin which is present at intermediate denaturant concentrations (see discussion to follow regarding Scheme 1).

Analytical ultracentrifugation clearly demonstrated that self-association of vitronectin does not occur in the presence of high concentrations of denaturant. It is not until the denaturant is removed by dialysis or dilution that self-association of the protein is observed. Formation of multimers of vitronectin has been previously demonstrated using either native polyacrylamide gel electrophoresis (11) or nonreducing SDS-polyacrylamide gel electrophoresis (12, 25, 26). Indeed, multimers were observed in the gel systems because the urea was separated from the protein during the course of electrophoresis and multimerization thus ensued in the electrophoretic buffer. The ultracentrifugation result agrees with previous use of size exclusion chromatography on denatured vitronectin in urea,

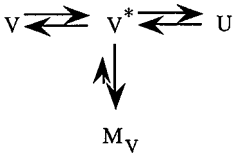

SCHEME 1

which gave an average elution volume characteristic of monomeric protein (11). As opposed to the size exclusion method, analytical ultracentrifugation allows for a rigorous determination of molecular weight under denaturing conditions since the equation describing the equilibrium distribution does not depend on hydrodynamic volume of the sedimenting species. From this analysis, it was established that the molecular weight of the denatured protein is equivalent to that of the vitronectin monomer.

Refolding curves exhibited hysteresis compared to unfolding curves in both GdnHCl and urea, indicating that different unfolding and refolding pathways were taken by vitronectin and certainly indicating that vitronectin was refolding to a structure distinct from the native fold of the protein. In striking contrast to the native monomer, the multimeric form of vitronectin can be unfolded with chemical denaturants and subsequently refolded in a reversible fashion. Treatment of the multimer with GdnHCl or urea dissociated it into constituent monomeric subunits, with a minor percentage of disulfide cross-linked species. Low concentrations of chemical denaturant were effective at dissociating the multimer into its constituent subunits; these concentrations of denaturant are lower than those required to unfold the protein subunits, indicating that the set of noncovalent interactions which contribute to the binding energetics between subunits are weaker than the sum of interactions that maintain the subunit in a compact folded form. Disulfide cross-linking upon denaturation of vitronectin has been previously observed to a variable extent (12). Since disulfide rearrangement occurs upon urea treatment of vitronectin, the covalent cross-linking between monomers within the multimer must be considered a formal possibility. Blocking of the available free sulfhydryls within native vitronectin with *N*-ethylmaleimide was used to demonstrate that multimers may form in the absence of intermolecular disulfides (11). The ultracentrifugation results demonstrate that any intermolecular disulfide bridging which occurs within the multimer when free sulfhydryls are not blocked does not substantially stabilize oligomers at higher levels than the dimer. Although disulfides clearly do not form uniform covalent bridges within the multimer, it is still possible that intramolecular disulfide rearrangement stabilizes an altered protein with a high propensity to self-associate. The contribution of disulfide rearrangement to the irreversible unfolding of vitronectin is evaluated in an accompanying study (27).

Based on the observation that both chaotropic agents and a basic peptide derived from the heparin-binding sequence located near the C terminus of vitronectin were effective at promoting self-association of vitronectin, Stockmann and co-workers (25) have concluded that both ionic and hydrophobic forces must be overcome to unfold vitronectin (25). In a similar vein, Hogasen and co-workers (12) propose that exposure of the heparin-binding site and a putative hydrophobic region on vitronectin are linked events as the protein unfolds, such that *in vitro* polymerization is driven by hydrophobic interactions and the heparin-binding site remains exposed on the surface of the multimer. In light of these speculations, it is most interesting to compare the unfolding behavior of vitronectin induced with GdnHCl and urea (Fig. 3). Although the midpoints are quite different, equal to 3.2 and 5.9 M, respectively, this is not surprising since GdnHCl is known to be a stronger denaturant. More unusual is the difference in the transition slopes, with a much sharper transition observed in GdnHCl, which is a salt in addition to a chaotrope. It is certainly envisioned that ionic and hydrophobic interactions make individual contributions to the overall folding of vitronectin, and perhaps disruption of hydrophobic and ionic interactions occur differently in the two chemical denaturants. The contribution of ionic interactions to folding of native and multimeric vitronectin is addressed in the accompanying article (27). Stockmann and co-workers (25) carry their argument further to suggest that the heparin-binding sequence within vitronectin is involved in multimerization of the protein, in spite of the fact that the multimer binds heparin quite effectively so that this region could not reasonably be envisioned to lie at the interface between subunits. This hypothesis is also considered in the following study (27).

From the perspective of protein folding, vitronectin has presented challenges as refolding of the protein is accompanied by self-association. The hysteresis between unfolding and refolding curves for vitronectin, along with characterization of the self-association process in this study, can be understood in relation to Scheme 1 which describes folding equilibria for vitronectin.

In the mechanism outlined in Scheme 1, V represents the native, monomeric form of vitronectin, V^* represents a partially unfolded intermediate structure, and U represents the fully unfolded monomer. The multimeric form of vitronectin is represented as M_v. This scheme is a minimal scheme, useful for interpreting the *in vitro* folding studies to date, although a more complicated mechanism is certainly possible. Loosening of the structure to a partially unfolded form at intermediate concentrations of denaturant results in an altered conformation of the protein which self-associates, with return to the original native fold of the protein virtually prohibited. Partially unfolded forms of vitronectin uniformly exhibit a propensity to self-associate, a property which is observed in many other cases of partially unfolded or "molten globule" forms of proteins with hydrophobic surfaces exposed. Under near physiological buffer conditions, unfolding/refolding of vitronectin is operationally irreversible so that the alternative pathway leading toward the multimeric form of the protein is highly favored. It thus appears that the form of vitronectin isolated as the native monomer is *not* the only stable fold, but rather represents one of at least two stable forms of the protein. Folding of plasma vitronectin, which occurs during synthesis and secretion from the liver into the circulation, apparently proceeds via a pathway in which folding to a monomeric form is favored. Protein folding within the cell differs from the *in vitro* refolding experiments, as it is assisted by molecular chaperones and targeted to cellular compartments by signal sequences on protein substrates, so that a degree of regulation is possible in which folding intermediates are prevented from or allowed to self-associate.[4] It appears that control of folding and self-association of vitronectin may be important for regulation *in vivo* since vitronectin found in extravascular sites is generally in the conformationally altered and multimeric form (24), and synthesis of vitronectin which occurs at extrahepatic sites (39) may be differentially regulated to produce either the monomeric or the multimeric form of the protein.

Acknowledgments—Many thanks to Liz Howell for helpful discussions and critical reading of the manuscript and to Mike Johnson for

[4] *In vitro* experiments in which the molecular chaperone *GroEL* was included upon initiation of refolding did not affect the observed self-association of refolded vitronectin into a multimeric form.

help in preparing the figures for publication. We appreciate Dean McNulty from the Protein Core Facility at SmithKline Beecham for the amino acid analysis on vitronectin.

REFERENCES

1. Preissner, K. T. (1989) *Blut* **59,** 419–431
2. Preissner, K. T., and Jenne, D. (1991) *Thromb. Haemostasis* **66,** 123–132
3. Preissner, K. T. (1991) *Annu. Rev. Cell Biol.* **7,** 275–310
4. Tomasini, B. R., and Mosher, D. F. (1991) *Prog. Hemostasis Thromb.* **10,** 269–305
5. Preissner, K. T., and Jenne, D. (1991) *Thromb. Haemostasis* **66,** 189–194
6. Kolb, W. P., and Muller-Eberhard, H. J. (1975) *J. Exp. Med.* **141,** 724–735
7. Dahlback, B., and Podack, E. R. (1985) *Biochemistry* **24,** 2368–2374
8. Yatohgo, T., Izumi, M., Kashiwagi, H., and Hayashi, M. (1988) *Cell Struct. Funct.* **13,** 281–292
9. Preissner, K. T., and Muller-Berghaus, G. (1986) *Eur. J. Biochem.* **156,** 645–650
10. Preissner, K. T., and Muller-Berghaus, G. (1987) *J. Biol. Chem.* **262,** 12247–12253
11. Bittorf, S. V., Williams, E. C., and Mosher, D. F. (1993) *J. Biol. Chem.* **268,** 24838–24846
12. Hogasen, K., Mollnes, T. E., and Harboe, M. (1992) *J. Biol. Chem.* **267,** 23076–23082
13. Tomasini, B. R., Owen, M. C., Fenton, J. W., II, and Mosher, D. F. (1989) *Biochemistry* **28,** 7617–7623
14. Tomasini, B. R., and Mosher, D. F. (1988) *Blood* **72,** 903–912
15. Hildebrand, A., Preissner, K. T., Muller-Berghaus, G., and Teschemacher, H. (1989) *J. Biol. Chem.* **264,** 15429–15434
16. Gechtman, Z., Sharma, R., Kreizman, T., Fridkin, M., and Shaltiel, S. (1993) *FEBS Lett.* **315,** 293–297
17. Chain, D., Korc-Grodzicki, B., Kreizman, T., and Shaltiel, S. (1991) *Biochem. J.* **274,** 387–394
18. Naski, M. C., Lawrence, D. A., Mosher, D. F., Podor, T. J., and Ginsburg, D. (1993) *J. Biol. Chem.* **268,** 12367–12372
19. Gebb, C., Hayman, E. G., Engvall, E., and Ruoslahti, E. (1986) *J. Biol. Chem.* **261,** 16698–16703
20. Wei, Y., Waltz, D. A., Rao, N., Drummond, R. J., Rosenberg, S., and Chapman, H. A. (1994) *J. Biol. Chem.* **269,** 32380–32388
21. Zanetti, A., Conforti, G., Hess, S., Martin-Padura, I., Ghibaudi, E., Preissner, K. T., and Dejana, E. (1994) *Blood* **84,** 1116–1123
22. Panetti, T. S., and McKeown-Longo, P. J. (1993) *J. Biol. Chem.* **268,** 11988–11993
23. Panetti, T. S., and McKeown-Longo, P. J. (1993) *J. Biol. Chem.* **268,** 11492–11495
24. Preissner, K. T., Grulich-Henn, J., Ehrlich, H. J., Declerck, P., Justus, C., Collen, D., Pannekoek, H., and Muller-Berghaus, G. (1990) *J. Biol. Chem.* **265,** 18490–18498
25. Stockmann, A., Hess, S., Declerck, P., Timpl, R., and Preissner, K. T. (1993) *J. Biol. Chem.* **268,** 22874–22882
26. Seiffert, D. (1995) *FEBS Lett.* **368,** 155–159
27. Zhuang, P., Li, H., Williams, J. G., Wagner, N., Seiffert, D., and Peterson, C. B. (1996) *J. Biol. Chem.* **270,** 14333–14343
28. Laemmli, U. K. (1970) *Nature* **227,** 680–685
29. Kawahara, K., and Tanford, C. (1966) *J. Biol. Chem.* **241,** 3228–3232
30. Brooks, I., Wetzel, R., Chan, W., Lee, G., Watts, D. G., Soneson, K. K., and Hensley, P. (1994) in *Modern Analytical Ultracentrifugation: Acquisition and Interpretation of Data for Biological and Synthetic Polymer Systems* (Shuster, T. M., and Laue, T. M., eds) pp. 15–36, Birkhauser, Boston
31. Brooks, I., Watts, D. G., Soneson, K. K., and Hensley, P. (1994) *Methods Enzymol.* **240,** 459–478
32. Royer, C. A., Mann, C. J., and Matthews, C. R. (1993) *Protein Sci.* **2,** 1844–1852
33. Pace, C. N., Shirley, B. A., and Thomsom, J. A. (1990) in *Protein Structure: A Practical Approach* (Creighton, T. E., ed) pp. 311–330, IRL Press, Oxford
34. Lakowicz, J. R. (1983) in *Principles of Fluorescence Spectroscopy*, pp. 258–297, Plenum Press, New York
35. Pitt, W. G., Fabrizius-Homan, D. J., Mosher, D. F., and Cooper, S. L. (1989) *J. Colloid Interface Sci.* **129,** 231–239
36. Steif, C., Weber, P., Hinz, H. J., Flossdorf, J., Cesareni, G., and Kokkinidis, J. (1993) *Biochemistry* **32,** 3867–3876
37. Munson, M., O'Brien, R., Sturtevant, J. M., and Regan, L. (1994) *Protein Sci.* **3,** 2015–2022
38. Neet, K. E., and Timm, D. E. (1994) *J. Protein Sci.* **3,** 2167–2174
39. Seiffert, D., Crain, K., Wagner, N. V., and Loskutoff, D. J. (1994) *J. Biol. Chem.* **269,** 19836–19842
40. Peterson, C. B. (1993) in *Biology of Vitronectins and Their Receptors* (Preissner, K. T., Rosenblatt, S., Kost, C., and Wegerhoff, J., eds) pp. 67–74, Elsevier, Amsterdam